Research on Performance Zoning of Asphalt Pavement in Xinjiang and Performance Grade(PG) of Asphalt Binder in Karamay

Chaofei Dong , Liqun Feng * , Yafeng Xu

Posted Date: 18 May 2023

doi: 10.20944/preprints202305.1307.v1

Keywords: Performance zoning; Superpave; Performance grade; Dynamic shear rheometer; Bending beam rheometer

Article

Research on Performance Zoning of Asphalt Pavement in Xinjiang and Performance Grade(PG) of Asphalt Binder in Karamay

Chaofei Dong [1], Liqun Feng [1,2,3,*] and Yafeng Xu [2,3]

[1] College of Architecture and Engineering, Xinjiang University, Urumchi, 830017, China
[2] Xinjiang Academy of Transportation Research, Urumchi, 830000, China
[3] Key Laboratory of Highway Engineering Technology in Arid Desert Zone Transportation Industry, Urumchi, 830000, China
* Correspondence: 15735103919@163.com; Tel.: +15-735-103-919

Abstract: Asphalt binder is a temperature sensitive material, whose performance is greatly affected by the climate change of the environment. Improper selection of asphalt will cause a lot of damage and affect the durability of the road. The establishment of asphalt pavement performance zoning in Xinjiang, a vast area with great temperature difference, will provide reference for the selection of asphalt suitability, the refinement of pavement design and the sustainable development of road engineering. In this study, 11 years of temperature data in Xinjiang region were collected and analyzed, and 98% reliability of pavement design temperature was used to draw a performance grading map of asphalt pavement in Xinjiang region based on ArcGIS platform. Finally, Xinjiang region was divided into 9 performance zones. At the same time, the performance grade (PG) of five kinds of asphalt binders in Karamay were explored. The result shows that there is little difference in continuous PG span between different matrix asphalt binders, the lower penetration grade, the better high temperature performance, the worse low temperature performance. After adding SBS modifier, the continuous PG span can be higher than the matrix asphalt in 20 °C. All these provide the basis for reasonable selection of asphalt binders in different areas of Xinjiang.

Keywords: performance zoning; superpave; performance grade; dynamic shear rheometer; bending beam rheometer

1. Introduction

Asphalt pavement has the advantages of low noise, easy maintenance, and fast construction, and is widely used in most high-grade roads in China [1–3]. Xinjiang is a vast territory and the climate varies greatly from region to region which makes the asphalt pavement in Xinjiang region is facing a severe test. Asphalt pavements are prone to rutting lesions under high-temperature driving loads [4], fatigue cracks under Intermediate temperature [5], experiencing prolonged repetitive driving loads, and transverse cracks under low-temperature cold environments [6,7], all of which seriously affect driving safety. Especially, global climate change over the years, the rise of pavement temperature, which puts forward higher requirements for the high and low temperature performance of asphalt roads [8].

The performance of asphalt pavement mainly depends on the performance of the asphalt binder material used for construction [9]. Asphalt binder has both viscous and elastic properties, showing soft viscous at high temperature and brittle behavior at low temperature [10]. Increasing the modulus of the asphalt binder can improve the load-bearing capacity of the pavement, thus reducing the occurrence of rutting [11–14]. There are usually two ways to increase the modulus of asphalt binder, one is to use asphalt with lower penetration grade, such as 50# or 30# matrix asphalt binder, the second is to add modified substances in the asphalt binder, such as SBS modifier and various high

 doi:10.20944/preprints202305.1307.v1

modulus agents [15]. Styrene-butadiene-styrene (SBS), as a copolymer, is often used as a modifier for asphalt binders to improve the bonding properties of the binder [16]. SBS modifiers can form a cross-linked network that improves the flexibility, elasticity and durability of the binder, this allows the asphalt better resist cracking, rutting and other forms of damage, thereby extending the life of the pavement [17]. In addition, the SBS modifier improves the viscosity of the asphalt, which results in better binding to the aggregate to form a more durable pavement [18]. However, the use of modified asphalt will greatly increase production costs, intensify the consumption of non-renewable resources, aggravate air pollution, and is not conducive to the sustainable development of the local economy [19,20], Xinjiang has abundant resources of low penetration asphalt grade, and the production cost is low. Due to the lack of comprehensive understanding of the performance of the asphalt with low penetration grade, the 90# matrix asphalt is still used for most of the asphalt pavement in Xinjiang. In summary, it is necessary to research the performance law of matrix asphalt with different penetration grades and the gap between them and SBS modified asphalt.

At present, the standard asphalt classification in China mainly adopts the penetration grade, this method is convenient, but can't accurately assess the high and low temperature performance of asphalt [21]. In contrast, the characterization methods based on performance grading can better simulate the actual conditions in which the asphalt is subjected [22,23].

The asphalt binder Performance grading (PG) system based on asphalt rheological properties is a product of the Strategic Highway Research Program (SHRP) in the United States [24]. In Superpave research, rheological analysis is widely used for road paving asphalt, including Dynamic Shear Rheometer (DSR), Bending Beam Rheometer (BBR) [25]. Among them, DSR test can provide a large amount of high temperature performance information, such as composite shear modulus (G*), phase angle (δ), rutting factor (G*/sinδ), and fatigue factor (G*·sinδ) parameters are used to quantify the high temperature rutting resistance and medium temperature fatigue resistance of asphalt binder [26]. The creep stiffness modulus S and m values obtained from BBR test are characterized the low temperature performance of asphalt.

According to the actual environment in which the asphalt pavement is located, the selection of suitable asphalt binder can not only enhance the durability [27,28], comfort and safety of asphalt pavement, but also achieve the purpose of economic and environmental protection, which is an effective way to achieve sustainable development. Therefore, many countries have conducted climate-based performance zoning studies and developed performance level zoning standards for asphalt pavements based on local climate, as a reference for asphalt suitability selection, so that asphalt pavement design can be adapted to the climatic environment of a region [29,30]. For example, the U.S. Strategic Highway Research Program (SHRP) proposed a method for classifying asphalt pavement performance grades (PG) based on high and low temperature indicators [31]. Asi et al. proposed a temperature-climate zoning method that divided Jordan into three zones based on the high and low temperatures of the pavement at 98% confidence level [32]. Hassam et al. used a data development model to predict high and low temperatures of asphalt pavements in Oman and proposed performance grades of asphalt binders for each region in Oman [33]. Saleh et al. converted road surface and pavement temperatures based on Superpave and LTTP projects to generate four asphalt performance grading zones for Egypt [34]. Mirza et al. recommend a SHRP model with 98% reliability that divides Pakistan into six PG grading zones [35]. Jitsangiam et al. divided northern Thailand into two grading zones by calculating the average temperature and standard deviation value at a 95% confidence level [36]. Salem et al. used the SHRP model with 50% reliability to classify the road PG grade of the Libyan desert into three zones [37]. Viola et al. developed an isoline map of pavement temperature in Italy based on the Superpave specification and considered the effects of climate change on pavement performance [38]. Cota et al. generated a PG grading chart of asphalt binders for Mexican based on temperature and elevation, which was used to determine the grade of asphalt binders required [39]. Zhang et al. proposed a temperature conversion formula for asphalt pavements in northeast China based on the SHRP method, established a PG climate zone in northeast China, and evaluated the high and low temperature performance of asphalt binders [9]. Zhao et al. proposed performance zoning indexes for different asphalt pavement layers in Inner Mongolia,

 doi:10.20944/preprints202305.1307.v1

China, and divided the asphalt pavement in Inner Mongolia into three main performance zones and six secondary performance zones, and verified them [40]. To sum up, the selection of asphalt is inseparable from the guidance of the performance zone of asphalt pavement, and it is necessary to establish the pavement performance classification map in Xinjiang region.

This paper is mainly through the collection and analysis of meteorological data in different regions of Xinjiang, to determine the environment in which the asphalt is located by pavement temperature, to establish a performance grade zoning chart of asphalt pavement in Xinjiang, and to propose the high and low temperature performance of asphalt to be used in different regions. Due to the wide application of Karamay asphalt in Xinjiang region, five kinds of asphalt were selected for PG grading study to determine the performance gap between matrix asphalt with different penetration grades and SBS modified asphalt, which provides reference and basis for suitable selection of asphalt binders in Xinjiang region, and also points out the direction for the sustainable development of asphalt pavement in Xinjiang region.

2. Generation performance grading maps of asphalt pavement for Xinjiang

2.1. Temperature data collection and analysis

The performance grade of Superpave asphalt binder is established based on the minimum and maximum pavement temperature expected on site. Due to the lack of pavement temperature data in Xinjiang, which was obtained by proposing a conversion model that based on the relationship between air temperature and pavement temperature. Therefore, the latitude and longitude of 84 stations in Xinjiang were collected and analyzed, as well as the average values of summer maximum temperature for seven consecutive days and extreme low temperature for seven consecutive days throughout the year for the past 11 years.

If the calculations are performed as an average of the temperatures, only 50% reliability levels of high and low temperature pavement temperatures can be obtained. Reliability is the percentage probability that the actual temperature does not exceed the design temperature over the course of a year, a higher percentage means lower risk. The maximum and minimum design temperatures at 98% reliability are calculated statistically. 98% reliability is two standard deviations from the average value, The calculations are as follows:

$$\text{T(max) at 98\%} = \text{X(High Temp)} + 2*\text{S(High Temp)}$$

$$\text{T(min) at 98\%} = \text{X(Low Temp)} - 2*\text{S(Low Temp)}$$

where the standard deviation value is determined by the calculation of Equation (1).

$$S = \sqrt{\frac{1}{N-1}\sum_{i=1}^{n}(X_i - X)} \quad (1)$$

Where X_i is a single temperature record, X is the average value of a set of temperatures, and N is the number of temperature records in a set.

These values are listed in Table 1, and the standard deviation values of maximum temperatures in different regions ranged from 1.1-2.8, while the standard deviation values of minimum temperatures ranged from 1.8-4.7, indicating that the maximum temperatures in the hot season had little difference in Xinjiang over the past decade, while the minimum temperatures fluctuated more in the cold season.

Preprints (www.preprints.org) | NOT PEER-REVIEWED | Posted: 18 May 2023 doi:10.20944/preprints202305.1307.v1

Table 1. Maximum and minimum temperatures and pavement design temperatures for stations in Xinjiang.

Station	Longitude(°)	Latitude (°)	Average of seven days average maximum temperature (℃)	Standard deviation	Maximum design temperature of road surface (℃)	Average of seven days average minimum temperature (℃)	Standard deviation	Minimum design temperature of road surface (℃)
Fuhai	87.48	47.11	38.0	2.2	65.50	-39.0	3.1	-31.83
Habahe	86.32	48.04	37.4	2.4	64.99	-37.8	4.1	-30.80
Buerjin	86.85	47.70	37.4	2.4	64.97	-39.0	3.8	-31.83
Jimunai	85.87	47.44	35.4	2.8	63.05	-34.8	4.1	-28.22
Fuyun	89.53	46.99	38.4	2.8	65.88	-41.0	4.1	-33.55
Qinghe	90.38	46.67	35.0	2.2	62.61	-42.2	3.4	-34.58
Tacheng	82.59	46.46	38.2	1.9	65.65	-33.2	4.1	-26.84
Emin	83.62	46.52	36.5	2.0	64.03	-36.5	4.5	-29.68
Yumin	82.98	46.20	38.0	2.2	65.44	-34.2	4.4	-27.70
Tuoli	83.60	45.94	34.8	1.9	62.37	-31.4	3.6	-25.29
Hebukesaier	85.72	46.79	32.2	1.5	59.95	-34.8	3.8	-28.22
Wusu	84.62	44.45	38.9	1.7	66.17	-30.6	2.5	-24.61
Kelamayi	84.77	45.59	39.5	1.7	66.83	-32.3	3.2	-26.07
Kuitun	84.89	44.45	38.9	1.6	66.17	-30.4	2.5	-24.43
Shawan	85.62	44.33	37.7	1.3	65.02	-31.5	3.1	-25.38
Manasi	86.20	44.29	39.1	1.8	66.35	-33.1	2.8	-26.76
Shihezi	86.00	44.18	39.2	1.5	66.44	-38.5	4.6	-31.40
Changji	87.30	44.02	40.3	2.1	67.48	-37.1	3.8	-30.19
Wulumuqi	87.61	43.79	37.7	2.1	64.98	-29.4	3.0	-23.58
Wujiaqu	87.54	44.17	41.0	2.1	68.16	-36.8	2.6	-29.94
Fukang	87.94	44.16	40.2	1.8	67.39	-32.5	3.0	-26.24
Miquan	87.68	43.97	40.0	1.9	67.19	-33.0	4.0	-26.67
Qitai	89.59	44.02	38.2	1.7	65.47	-37.1	3.3	-30.19
Jimusaer	89.18	44.00	38.2	1.6	65.47	-32.2	3.2	-25.98
Mulei	90.28	43.83	34.4	1.8	61.83	-32.6	3.9	-26.33
Balikun	93.01	43.59	33.0	2.0	60.48	-35.0	3.3	-28.39
Yiwu	94.69	43.25	32.8	1.7	60.26	-31.3	2.6	-25.21
Hami	93.44	42.78	41.4	1.4	68.43	-26.6	2.6	-21.17
Tulufan	89.18	42.93	46.2	1.3	73.02	-19.8	2.6	-15.32
Shanshan	90.21	42.86	43.8	1.4	70.73	-22.5	2.2	-17.64
Tuokesun	88.65	42.79	46.5	1.6	73.30	-20.4	2.0	-15.84
Hejing	86.39	42.31	36.7	1.3	63.90	-24.2	1.9	-19.10
Heshuo	86.86	42.26	36.6	1.2	63.80	-25.6	2.2	-20.31

 doi:10.20944/preprints202305.1307.v1

Yanqi	86.57	42.05	37.2	1.5	64.36	-26.0	2.6	-20.65
Bohu	86.63	41.98	36.5	1.1	63.69	-25.6	2.7	-20.31
Kuerle	86.06	41.68	38.7	1.7	65.76	-20.8	1.9	-16.18
Yuli	86.25	41.33	39.3	1.3	66.30	-24.3	2.5	-19.19
Ruoqiang	88.17	39.02	42.3	1.5	68.96	-22.3	1.9	-17.47
Qiemo	85.53	38.14	40.2	1.4	66.87	-21.6	1.8	-16.87
Minfeg	82.68	37.06	40.6	1.7	67.15	-21.1	2.4	-16.44
Yutian	81.95	36.45	39.2	1.4	65.75	-19.7	2.3	-15.24
Cele	80.78	37.04	40.0	1.5	66.57	-19.2	2.3	-14.81
Hetian	79.94	37.12	39.1	1.5	65.72	-18.4	2.7	-14.12
Moyu	79.71	37.31	38.9	1.3	65.55	-20.8	2.1	-16.18
Pishan	78.29	37.62	39.3	1.5	65.96	-19.9	2.5	-15.41
Tashiuergan	75.23	37.77	30.2	1.5	57.29	-28.7	1.8	-22.97
Yecheng	77.42	37.89	37.7	1.4	64.46	-20.0	2.8	-15.49
Zepu	77.26	38.20	38.5	1.4	65.25	-20.1	2.3	-15.58
Shache	77.25	38.45	38.8	1.5	65.56	-19.5	2.5	-15.06
Maigaiti	77.64	38.95	39.1	1.4	65.90	-19.8	2.3	-15.32
Yingjisha	76.17	38.93	38.6	1.2	65.42	-20.8	3.1	-16.18
Yuepuhu	76.77	39.23	40.1	1.3	66.88	-20.7	2.5	-16.10
Jiashi	76.73	39.50	39.4	1.3	66.24	-20.6	2.5	-16.01
Shule	76.05	39.41	38.3	1.5	65.18	-19.5	2.5	-15.06
Shufu	75.86	39.37	37.9	1.2	64.79	-19.5	2.6	-15.06
Aketao	75.95	39.15	37.6	1.2	64.48	-21.8	2.8	-17.04
Kashi	75.99	39.46	37.8	1.3	64.70	-20.6	2.8	-16.01
Wuqia	75.25	39.71	32.4	1.5	59.57	-23.6	1.9	-18.59
Atushi	76.16	39.73	39.0	1.4	65.87	-18.5	2.5	-14.20
Bachu	78.59	39.78	39.0	1.2	65.88	-20.0	2.2	-15.49
Tumukeshu	79.13	39.85	39.2	1.3	66.08	-16.4	2.7	-12.40
Aheqi	78.44	40.93	33.9	1.6	61.11	-24.2	2.2	-19.10
Keping	79.05	40.51	38.7	1.2	65.66	-22.8	2.8	-17.90
Awati	80.37	40.64	37.8	1.6	64.81	-21.5	2.3	-16.78
Wushi	79.22	41.21	35.1	1.2	62.28	-24.4	2.9	-19.28
Wensu	80.24	41.27	37.6	1.4	64.67	-22.0	2.6	-17.21
Akesu	80.26	41.17	37.9	1.2	64.95	-21.5	2.2	-16.78
Alaer	81.29	40.54	38.4	1.2	65.37	-23.5	2.7	-18.50
Shaya	83.19	41.05	39.0	1.5	65.99	-20.8	2.5	-16.18
Kuche	82.96	41.71	37.4	1.3	64.52	-21.9	2.5	-17.13
Xinhe	82.63	41.55	37.6	1.3	64.70	-22.6	2.5	-17.73
Baicheng	81.84	41.82	36.5	1.4	63.67	-27.0	3.2	-21.51
Luntai	84.25	41.77	39.1	1.5	66.15	-24.3	3.0	-19.19
Zhaosu	81.13	43.15	29.8	1.8	57.39	-30.1	3.0	-24.18
Tekesi	81.83	43.21	34.3	1.5	61.69	-29.6	3.3	-23.75
Gongliu	82.23	43.48	36.7	1.5	64.00	-30.1	3.5	-24.18

Preprints (www.preprints.org) | NOT PEER-REVIEWED | Posted: 18 May 2023 doi:10.20944/preprints202305.1307.v1

Xinyuan	83.26	43.42	36.5	1.5	63.80	-25.3	3.4	-20.05
Nileke	82.51	43.80	35.9	1.6	63.26	-32.0	3.5	-25.81
Yining	81.33	43.91	38.2	1.7	65.46	-31.2	4.2	-25.12
Chabuchaer	81.15	43.84	38.7	1.6	65.94	-33.7	4.7	-27.27
Huocheng	80.87	44.05	38.7	1.6	65.95	-30.7	3.7	-24.69
Wenquan	81.03	44.97	33.4	1.9	60.96	-31.6	2.0	-25.47
Bole	82.10	44.93	38.8	1.5	66.11	-32.8	2.7	-26.50
Jinghe	82.88	44.60	39.5	1.5	66.76	-33.2	2.7	-26.84

Since the temperature data with 98% reliability obtained cannot cover all areas , the spatial difference method is generally used to predict the characteristics of unknown geographical areas by using known partial spatial information, which is also the biggest advantage of the spatial difference method. The inverse distance weighting (IDW) method, as a fast and accurate deterministic interpolation method, can calculate weights from the distances of known and unknown points. In space, things that are closer to each other are more similar than things that are farther away from each other. When predicting values for any unmeasured location, the inverse distance weighting method uses the measurements around the predicted location. The measurements closest to the predicted location are assumed to have a greater influence on the predicted value than measurements farther away from the predicted location. The function is:

$$Z = \frac{\sum_{i=1}^{n} \frac{1}{D_i^p} Z_i}{\sum_{i=1}^{n} \frac{1}{D_i^p}} \tag{2}$$

Where Z is the interpolation point value; Z_i is the observation value of the ith sample point; D_i^p is the distance between the ith observation point and the interpolation point; n is the number of samples; p is the power of the distance.

In ArcGIS, longitude and latitude of 84 meteorological points and 98% reliability of temperature data were input, and IDW spatial interpolation method was used to obtain the high temperature isotherm and low temperature isotherm in Xinjiang respectively, as shown in Figure 1a,b. The high temperature in different areas of Xinjiang under 98% reliability ranges from 29.8°C to 46.5°C, and the low temperature ranges from -16.4°C to -42.2°C. Most of the areas are under the climate conditions of hot summer and cold winter.

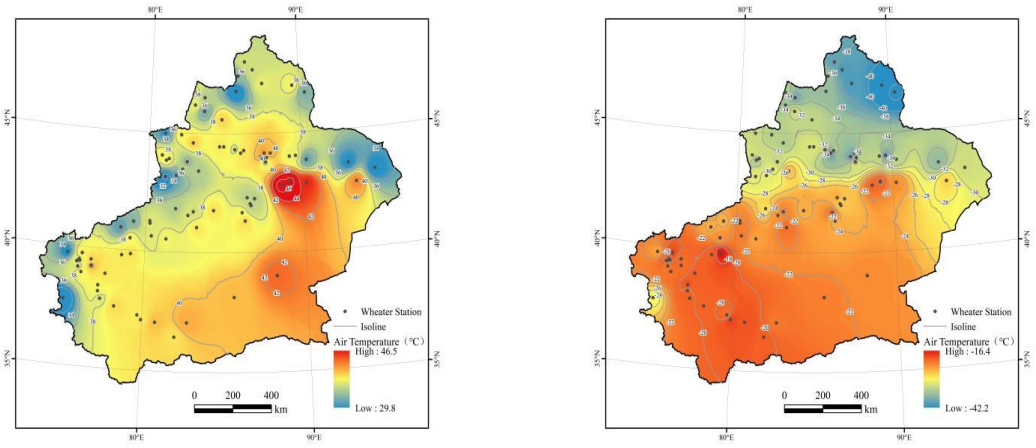

(**a**) (**b**)

Figure 1. Temperature map with 98% reliability in Xinjiang region. (**a**) high temperature isotherm map; (**b**) low temperature isotherm map.

Preprints (www.preprints.org) | NOT PEER-REVIEWED | Posted: 18 May 2023 doi:10.20944/preprints202305.1307.v1

2.2. Pavement temperature calculation

According to the theory of net heat flow and energy balance, the road temperature conversion model in Xinjiang is proposed in Xinjiang Highway Asphalt Pavement Design Instruction Manual. The maximum air temperature is converted to the maximum design temperature at 20 mm below the road surface as defined by formula (2) and the minimum air temperature is converted to the minimum design temperature of the road surface as defined by formula (3).

$$T_{20mm} = (T_{air} - 0.00618Lat^2 + 0.2289Lat + 42.2) \times 0.9545 - 17.78 \quad (3)$$

Where T_{20mm} is the high temperature design temperature of the pavement at 20 mm below the road surface, °C; T_{air} is the maximum temperature with 98% reliability, °C; Lat-geographic dimension, °.

$$T_{min} = 0.8597T_{air} + 1.7 \quad (4)$$

Where T_{min} is the low temperature design temperature of the road surface, °C; T_{air} is the minimum temperature with 98% reliability, °C.

By inputting the high and low temperature data with 98% reliability into the pavement temperature conversion model, the maximum and minimum design temperature of the pavement can be obtained. The specific temperature values are listed in Table 1. The isotherms of maximum temperature and minimum temperature of pavement temperature were generated respectively, as shown in Figure 2a,b. The extreme maximum temperature reached 73.3°C in some areas, the minimum extreme maximum temperature was 57.3°C, and the extreme minimum temperature of pavement was 34.6°C.

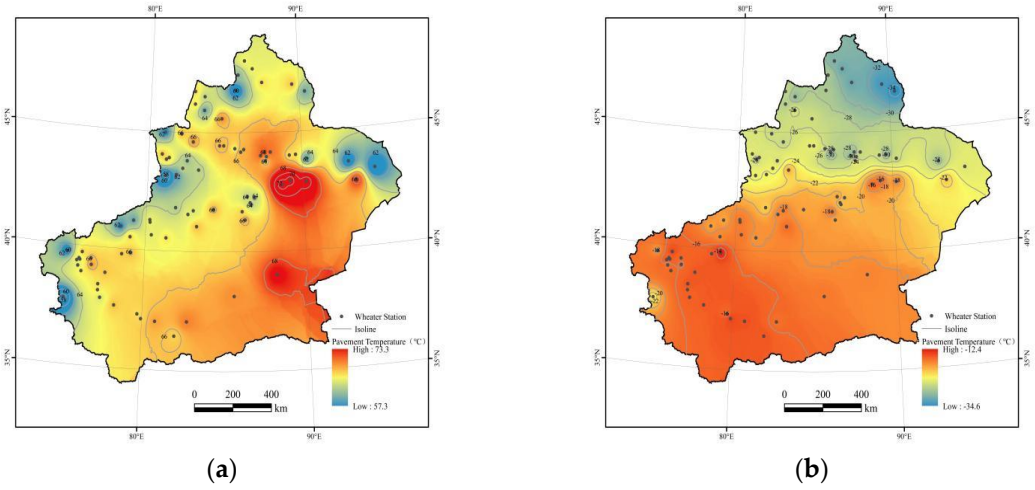

(**a**) (**b**)

Figure 2. Pavement temperature map with 98% reliability in Xinjiang region. (**a**) high temperature isotherm map; (**b**) low temperature isotherm map.

2.3. Generating performance grading maps for Xinjiang

The performance classification of asphalt pavement in Xinjiang was drawn by analyzing the pavement temperature, and finally nine zones of PG grading were divided, which are PG76-22, PG70-16, PG70-22, PG70-28, PG70-34, PG64-22, PG64-28, PG64-34, PG58-40, as shown in the Figure 3. As can be seen from the Figure 3, the four divisions with the largest area share are PG70-16, PG70-22, PG70-28, and PG70-34, indicating that the pavement temperature can reach 70°C in most areas of Xinjiang during the hot season. The asphalt used in different performance zones in the Figure 3 needs to meet the corresponding requirements of maximum and minimum design temperature, so as to ensure the durability of the road, reliability, but also provides a basis for the refined design of asphalt pavements in Xinjiang.

Preprints (www.preprints.org) | NOT PEER-REVIEWED | Posted: 18 May 2023 doi:10.20944/preprints202305.1307.v1

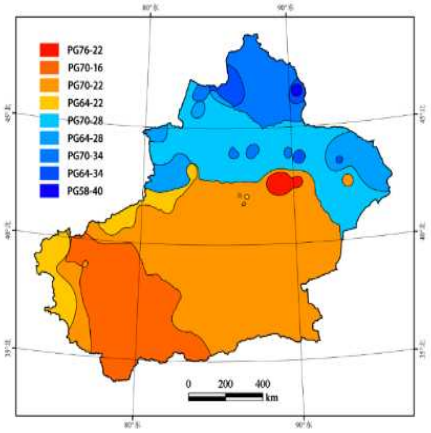

Figure 3. Asphalt pavement performance grading maps in Xinjiang region.

3. Materials and Methods

3.1. materials

In this paper, four different penetration grades of matrix asphalt binders(90#, 70#, 50#, 30#) and one SBS modified asphalt binder(modified by 90# matrix asphalt) were researched. All five asphalt binders were provided by PetroChina Karamay Petrochemical Co. SBS modified asphalt binder is prepared by a new chemical method. The chemical modified stabilizer is added to make the chemical condensation and crosslinking reaction between SBS modified asphalt binder and matrix asphalt binder, improve the compatibility between SBS polymer and matrix asphalt, and improve the high temperature stability and storage stability of SBS modified asphalt binder. The basic performance indexes of the five asphalt binders are shown in Table 2. The test procedures are operated in accordance with the specification JTG E20-2011 [41], and all the indicators of the five asphalt binders meet the specification JTG F40-2004 [42].

Table 2. Basic performance index of five asphalts binders.

Technical Indexes		Unit	90#	70#	50#	30#	SBS
Penetration (25°C,100g,5s)		0.1mm	87	72	55.8	32.8	76
Penetration index, PI		-	-1.11	-0.34	-0.22	-0.02	0.53
Softening point, TR&B		°C	45.3	49.0	50.2	55.6	65.6
Ductility(15°C,5cm/min)		cm	>100	>100	>100	61	/
Ductility(10°C,5cm/min)		cm	>100	>100	>100	8	42.1[a]
Density@15°C		g/cm^3	0.983	0.986	0.985	0.986	0.985
Dynamic viscosity@60°C		Pa·S	252	421	879	1783	1.977[b]
Solubility		%	0.983	0.986	0.985	0.986	0.985
After RTFOT (163°C 85min)	Mass change	%	-0.035	-0.035	-0.064	-0.088	-0.185
	Penetration ration @25°C	%	77	75	74	77	84
	Ductility(15°C,5cm/min)	cm	>100	>100	27	9	/
	Ductility(10°C,5cm/min)	cm	40	11	/	/	25.1[c]

Note: [a] The ductility test of SBS modified asphalt binder (unaged) is the results at 5°C. [b] The viscosity is Brookfield rotational viscosity at 135°C. [c] The ductility test of SBS modified asphalt binder (RTFOT aged) is the results at 5°C.

 doi:10.20944/preprints202305.1307.v1

3.2. Performance methods

The performance of five asphalt binders was evaluated according to the Superpave binder specification [43]. Dynamic shear rheometer (DSR) test and bending beam rheometer (BBR) test were used to evaluate the high temperature rutting resistance, medium temperature fatigue resistance, and low temperature cracking resistance of the matrix asphalt and SBS modified asphalt with different penetration grades. Finally, the PG grade of the asphalt binder was obtained. The PG grade is used to adapt the performance grades of asphalt required for different asphalt pavements in Xinjiang region.

3.2.1. Dynamic shear rheometer (DSR)

The high-temperature performance of the five asphalts can be measured by dynamic shear rheometer (DSR). The dynamic shear rheometer (DSR) is shown in the Figure 4. The test parameters such as the composite shear modulus (G*) and the phase angle (δ) can be obtained by testing the relationship between the applied stress and the measured strain. The PG high-temperature performance of asphalt binder is generally characterized by the rutting factor (G*/sinδ) of the unaged asphalt binder and RTFOT short-term aged asphalt binder.

Figure 4. Dynamic shear rheometer (DSR).

The test was conducted in the temperature range of 52°C~88°C with an increment of 6℃, and a 25mm diameter rotor selected for the parallel plate geometry and sample height equal to 1mm. When the temperature reaches equilibrium, the equipment is automatically tested at a frequency of 10 rad/s and selected stress target values. The test is automatically terminated when the rutting factor (G*/sinδ) of the unaged asphalt binder is less than 1 kPa and the rutting factor (G*/sinδ) of the RTFOT aged asphalt binder is less than 2.2 kPa.

The Intermediate temperature fatigue performance of asphalt is generally characterized by fatigue factor (G*·sinδ) of RTFOT+PAV aged asphalt binder. PAV aging container is shown in the Figure 5. The test temperatures are 19℃, 22℃, 25℃, 28℃, and an 8mm diameter rotor selected for the parallel plate geometry and sample height equal to 2mm. Asphalt binder with PG grading of PGm-n requires a fatigue factor (G* · sinδ) of less than 5000 kPa at (m-n)/2+4°C to meet the specification.

Preprints (www.preprints.org) | NOT PEER-REVIEWED | Posted: 18 May 2023 doi:10.20944/preprints202305.1307.v1

Figure 5. PAV aging container.

3.2.2. Bending beam rheometer (BBR)

The bending beam rheology (BBR) test can accurately evaluate the ability of asphalt to resist cracking under low temperature conditions. The bending beam rheology (BBR) is shown in the Figure 6. The parameters such as creep stiffness modulus S and m-value of asphalt binder are calculated by applying a constant load and measuring the deflection. The S represents the stiffness of the material and m-value represents the stress dissipation/ relaxation capacity due to temperature change. The lower the S value and the higher the m-value, the better the low temperature performance of the asphalt binder.

Figure 6. Bending beam rheology (BBR).

Trabecular bending samples of five kinds of asphalt binders were prepared, and the sample size was 127 mm × 12.7 mm × 6.35 mm. In the Superpave specification, the test temperature will be increased by 10℃, and the stiffness modulus with loading time of 60S will be replaced by the stiffness modulus after loading at the minimum pavement design temperature of 2h. The specification requires the stiffness modulus (S) with loading time of 60S is less than 300MPa, and m-value is greater than 0.3. At this time, the temperature will be reduced by 10℃, which is the minimum temperature for asphalt to meet the low temperature requirements. The tests were conducted at low temperatures of -12°C, -18°C and -24°C, and the samples were loaded continuously for 240 s. During the test, the creep stiffness modulus (S) and creep rate m-value of trabecular specimens were automatically collected by the computer through the sensor.

Preprints (www.preprints.org) | NOT PEER-REVIEWED | Posted: 18 May 2023 doi:10.20944/preprints202305.1307.v1

4. Results and discussion

4.1. High-temperature PG

The composite shear modulus (G*) and phase angle (δ) of the five asphalt binders after unaged and RTFOT short-term aging are shown in Figure 7a–d.

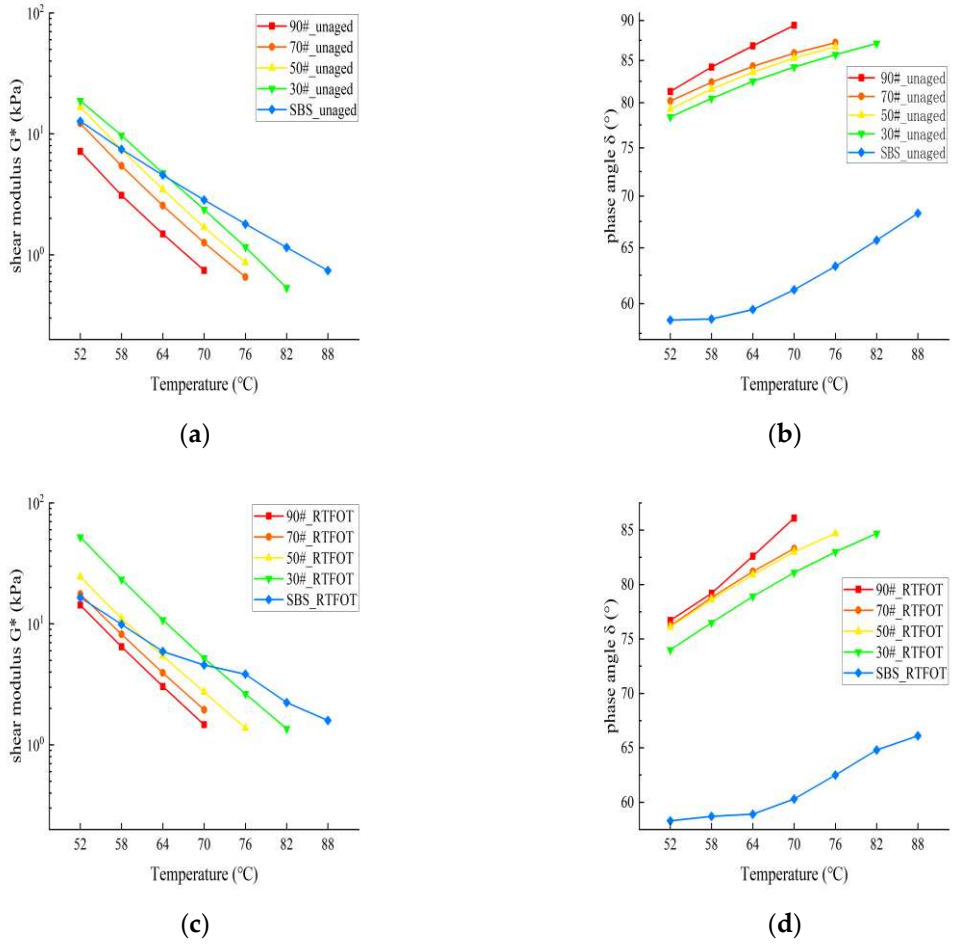

Figure 7. The composite shear modulus (G*) and phase angle (δ) at unaged and RTFOT aged condition. (**a**) G* at unaged condition; (**b**) δ at unaged condition; (**c**) G* at RTFOT aged condition; (**d**) δ at RTFOT aged condition.

The composite shear modulus (G*) represents a measure of the total resistance of the material during repeated shear deformation. The larger the value of G*, the stronger the ability of the asphalt to resist shear deformation. The lower the penetration grade of the base asphalt, the greater the G* value, and the unaged SBS modified asphalt has better shear deformation resistance than the matrix asphalt binder when the temperature reaches 70℃. Phase angle (δ) indicates the proportion of viscous components of asphalt binder, the larger the phase angle (δ), the larger the proportion of viscous components of asphalt binder. The smaller the proportion of elastic components, the weaker the ability to recover after deformation. The large difference in phase angle δ between SBS modified asphalt binder and matrix asphalt binder is mainly due to the addition of SBS modifier, which makes the asphalt binder exhibit more elastic properties.

After experiencing RTFOT short-term aging, the composite shear modulus G* of all five asphalt binders increased to varying degrees, and 30# is the most obvious, indicating that short-term aging increases the ability of the asphalt binder to resist shear deformation. At the same time, the phase Angle decreases to varying degrees, indicating that short-term aging will increase the proportion of elastic components in asphalt binder. In summary, short-term aging will enhance the ability of

Preprints (www.preprints.org) | NOT PEER-REVIEWED | Posted: 18 May 2023 doi:10.20944/preprints202305.1307.v1

asphalt binder to resist rutting deformation, and has the greatest effect on the asphalt binder of low penetration grade.

The rutting factor (G*/sinδ) is used in the Superpave specification to determine the high PG temperature of the asphalt binder. The benchmarks for rutting parameters equal to or higher than 1.0 kPa and 2.2 kPa are adopted for unaged and RTFOT aged, respectively. The rutting factors of the five asphalt binders are shown in Figure 8a,b.

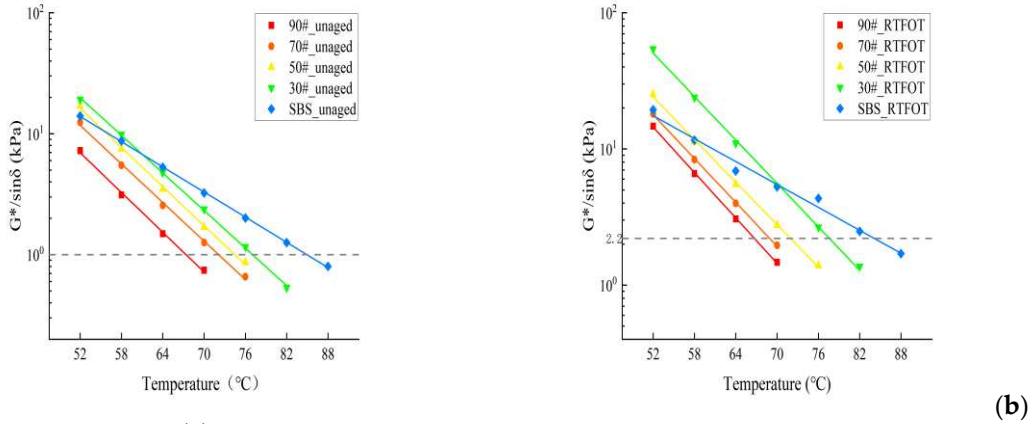

(**a**) (**b**)

Figure 8. The rutting factor (G*/sinδ) of five asphalt binders. (**a**) unaged; (**b**) RTFOT aged.

As shown in Figure 8a,b. The high-temperature PG of the five asphalt binders (90#, 70#, 50#, 30#, and SBS) are 66.7°C, 69.0°C, 72.1°C, 76.8°C, and 83.2°C, respectively. The high temperature rutting resistance of the five asphalt binders is SBS＞30#＞50#＞70#＞90#.

Compared with 90# matrix asphalt, the continuous gradation temperature of 70#, 50# and 30# increased by 2.3℃, 5.4℃ and 10.1℃, respectively, mainly because there are more elastic components in the asphalt binder with low penetration grade, while the continuous gradation temperature of SBS modified asphalt increased by 16.5℃. It shows that SBS modifier can significantly improve the high temperature rutting resistance of asphalt binder.

4.2. Intermediate temperature PG

The composite shear modulus (G*) and phase angle (δ) of the five asphalt binders under RTFOT + PAV aging conditions are shown in Figure 9a,b.

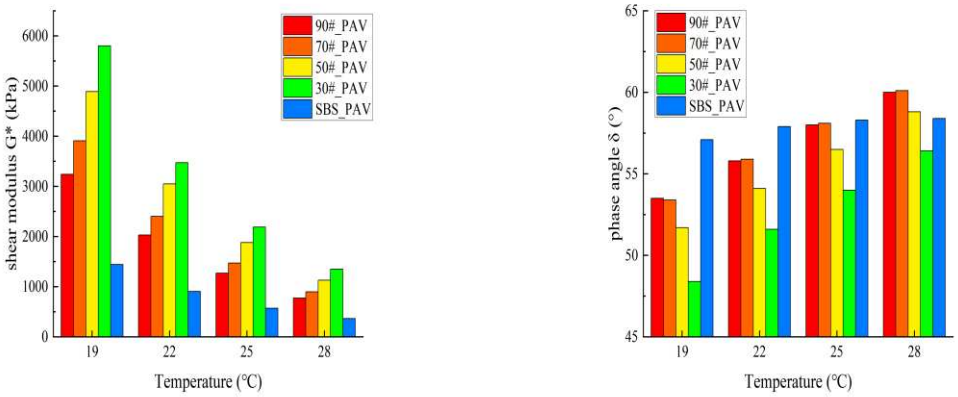

Figure 9. The rutting factor (G*/sinδ) of five asphalt binders. (**a**) unaged; (**b**) RTFOT aged.

From Figure 9a,b, it can be seen that the composite shear modulus of the five asphalt binders gradually decreases with increasing temperature, and the phase angle gradually becomes larger with

 doi:10.20944/preprints202305.1307.v1

increasing temperature. The lower the penetration grade of the matrix asphalt, the higher the composite shear modulus and the smaller the phase angle, which is consistent with the law of the unaged asphalt under high temperature conditions.

Compared with the matrix asphalt, SBS modified asphalt binder has a lower composite shear modulus, and the phase angle is greater than the remaining four matrix asphalt binders before 25°C. After the temperature reaches 25°C, the phase angle is gradually smaller than that of each matrix asphalt binder, and the phase angle of SBS modified bitumen changes the least at the four temperatures, indicating that its ability to resist shear deformation is less affected by temperature.

According to the Superpave specification, the fatigue factor (G*·sinδ) was used as the fatigue parameter of the asphalt binder, as shown in Figure 10, which was limited to 5.000 kPa as the performance criterion of RTFOT+ PAV aging binder at intermediate temperatures. It can be observed that at the intermediate temperature, the fatigue factor size of the five asphalt binders is regular: SBS > 90# > 70# > 50# > 30#, indicating that the lower the penetration grade of the matrix asphalt, the less flexible the asphalt is, the worse the fatigue performance SBS modified asphalt has better fatigue performance than the matrix asphalt.

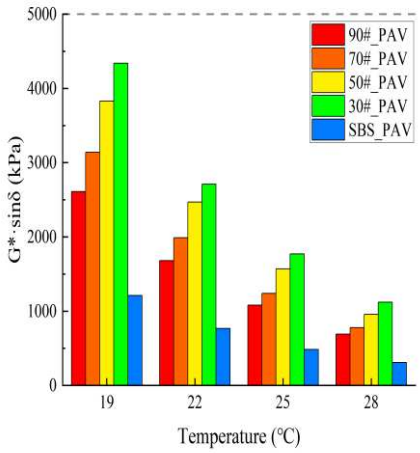

Figure 10. The fatigue factor (G*·sinδ) of five asphalt binders.

Overall, the fatigue factors of all five asphalt binders are much less than 5.000 kPa at the regulated temperature, indicating that the asphalt binder from Karamay has good fatigue resistance.

4.3. Low temperature PG

The creep stiffness modulus S and m-values calculated from the BBR tests at three different temperatures (-12°C, -18°C and -24°C) with a loading time of 60 s are shown in Figure 11a,b, respectively. As shown in Figure 11a,b, The 90# and 70# asphalt binders meet the Superpave requirement at -18°C, 50# and 30# asphalt binders meet the Superpave requirement at -12°C, and SBS modified asphalt reaches the Superpave limit at the temperature of -24°C.

Preprints (www.preprints.org) | NOT PEER-REVIEWED | Posted: 18 May 2023 doi:10.20944/preprints202305.1307.v1

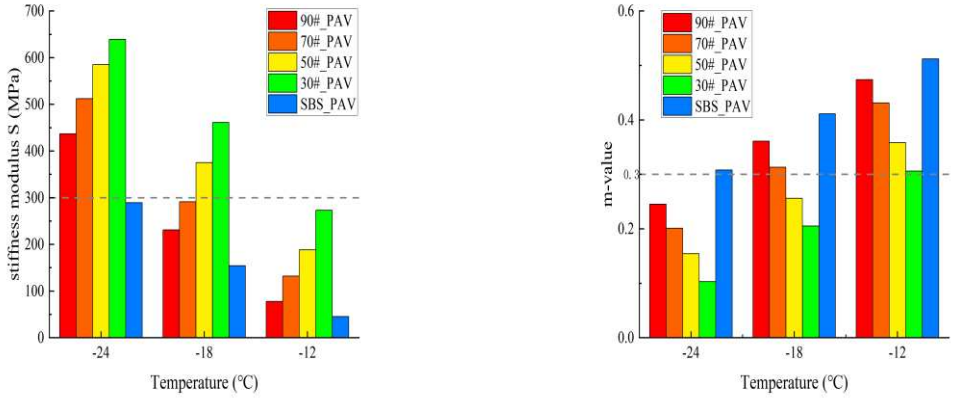

(**a**) (**b**)

Figure 11. The creep stiffness modulus S and m-values of five asphalt binders. (**a**) stiffness modulus S; (**b**) m-values.

The lower the modulus of stiffness, the lower the temperature stress of the material under the same temperature shrinkage strain, indicating that the low temperature cracking resistance of the material is stronger. At the same temperature, among the five asphalts, SBS modified asphalt has the lowest stiffness modulus and 30# asphalt has the highest stiffness modulus. The low temperature cracking resistance of the five asphalt binders is SBS > 90# > 70# > 50# > 30#. Compared with 90# base asphalt, the continuous grading temperature of 70#, 50# and 30# base asphalt decreased by 1.8℃, 4.6 ℃ and 7.6℃, respectively, mainly because of the increase of elastic component in the low penetration grade asphalt binder, while the continuous grading temperature of SBS modified asphalt increased by 4.3℃, which indicates that the addition of SBS modifier can improve the low temperature performance of asphalt binder.

4.4. Intermediate temperature PG

The full performance grades, continuous performance grades, the difference between continuous high PG and continuous low PG of the five asphalt binders evaluated in this paper are shown in Table 3.

Table 3. PG grading of five asphalt binders.

Parameter	Condation	Specfication	PG				
			90#	70#	50#	30#	SBS
G*/sinδ	Original	≥1kPa	67.5	71.8	74.4	76.8	84.9
G*/sinδ	RTFOT	≥2.2kPa	66.7	69.0	72.1	77.6	83.2
	Upper PG		64	64	70	76	82
G*·sinδ	PAV	≤5000kPa	22	22	28	31	28
	Intermediate PG		22	22	28	31	28
S	PAV	≤300MPa at 60 sec	-30.0	-28.2	-25.6	-22.9	-34.3
m-value	PAV	≥0.3kPa at 60 sec	-31.3	-28.7	-25.4	-22.4	-34.5
	Lower PG		-28	-28	-22	-22	-34
	PG		64-28	64-28	70-22	76-22	82-34

 doi:10.20944/preprints202305.1307.v1

Continuous PG	66.7-30	69-28.2	72.1 - 25.4	76.8-22.4	83.2-34.3
Difference between cont. high and cont. low PG	96.7	97.2	97.5	99.2	117.5

For the matrix asphalt binder, the lower the penetration grade, the better the high temperature performance and the higher the PG high temperature grade, but the difference between high continuous PG and low continuous PG for different matrix asphalt is not significant, indicating that the matrix asphalt has improved its high temperature performance while the low temperature performance also decreases accordingly.

According to the full performance grade for classification, 90# and 70# asphalt binders in the same PG range, indicating that in some cases, the PG grade for asphalt performance is not fine enough to distinguish, it is recommended to combine the penetration grade and continuous PG classification together for reference.

Due to the addition of modifier, SBS modified asphalt can not only improve the high temperature performance, but also improve the low temperature performance, so it has a larger continuous PG span and can adapt to a wider temperature domain. In the area with a larger temperature difference, SBS modified asphalt can be considered.

5. Summary and conclusions

By drawing a performance grading map of asphalt pavement in Xinjiang, and also researching the PG grading of five asphalt binders in Karamay, aiming to provide guidance and reference for the selection of asphalt in different areas of Xinjiang to ensure that it is more adaptable to local climatic conditions, the following conclusions were mainly obtained according to the results of the study:

(1) The asphalt pavement performance grading map of Xinjiang region divides Xinjiang into nine sub-districts, which indicates that the climate varies significantly in different areas of Xinjiang. The four partitions with the largest area share are PG70-16, PG70-22, PG70-28, and PG70-34, indicating that the pavement temperature is close to 70°C in most areas of Xinjiang during the high temperature season.

(2) For the five partitions with continuous PG range over 92°C (PG76-22, PG70-28, PG70-34, PG64-34, PG58-40), modified bitumen is recommended to ensure that the pavement performance needs can be met. The remaining four subdivisions are recommended to use matrix asphalt to meet the performance requirements in order to achieve economic and environmental protection.

(3) The lower the needle penetration grade of the matrix asphalt, the better the high temperature performance, the worse the low temperature performance, but overall the continuous PG span difference is not large, SBS modified asphalt continuous PG span can be higher than the matrix asphalt about 20 °C.

(4) For the case that different needle penetration grades of asphalt have the same PG grade, it is recommended to combine the needle penetration grade and continuous PG range together for reference.

Author Contributions: Conceptualization, Liqun Feng.; validation, Liqun Feng.; formal analysis, Chaofei Dong.; resources, Liqun Feng.; writing—original draft preparation, Chaofei Dong.; writing—review and editing, Chaofei Dong.; supervision, Liqun Feng; project administration, Yafeng Xu.; funding acquisition, Liqun Feng and Yafeng Xu. All authors have read and agreed to the published version of the manuscript.

Funding: This research was funded by "customized" asphalt road performance of Xinjiang Institute of Transport Science , grant number 2021-KT-01.

Data Availability Statement: Data will be made available on request.

Acknowledgments: We would like to thank the anonymous reviewers for their constructive feedback and detailed suggestions.

Conflicts of Interest: The authors declare no conflict of interest.

References

1. Haoran Zhu, Gang Xu, Minghui Gong, Jun Yang. Recycling long-term-aged asphalts using bio-binder/plasticizer-based rejuvenator. *Construction and Building Materials*. **2017**,*147.117-129.*
2. İslam Gökalp, Volkan Emre Uz. Utilizing of Waste Vegetable Cooking Oil in bitumen: Zero tolerance aging approach. *Construction and Building Materials*. **2019**,*227, 116695.*
3. Yan K Z, Hong Z, You L Y, et al. Influence of ethylene-vinyl acetate on the performance improvements of low-density polyethylene-modifeied bitumen. *Journal of Cleaner Production*. **2021**,*278,123865.*
4. Yinfei Du, Jiaqi Chen, Zheng Han, Weizheng Liu. A review on solutions for improving rutting resistance of asphalt pavement and test methods. *Construction and Building Materials*. **2018**,*168.*
5. Wenyao Liu, Kezhen Yan, Dongdong Ge, Ming Chen. Effect of APAO on the aging properties of waste tire rubber modified asphalt binder. *Construction and Building Materials*.**2018,***175.*
6. Xing, M. Yang, H. Zhao, Z. Yu, T. Effect of Asphalt Pavement Base Layers on Transverse Shrinkage Cracking Characteristics. *Sustainability*. **2023**, *15, 7178.*
7. Kun Zhang, John Kevern. Review of porous asphalt pavements in cold regions: the state of practice and case study repository in design, construction, and maintenance. *Journal of Infrastructure Preservation and Resilience*,**2021**,*2.*
8. Miao, Y. Sheng, J. Ye, J. An Assessment of the Impact of Temperature Rise Due to Climate Change on Asphalt Pavement in China. *Sustainability*. **2022,** *14, 9044.*
9. Haitao Zhang, Mingyang Gong, Yingli Huang, Miomir Miljković. Study of the high and low-temperature behavior of asphalt based on a performance grading system in Northeast China. *Construction and Building Materials*,**2020**,*254.*
10. Hamid, A. Baaj, H. El-Hakim, M. Temperature and Aging Effects on the Rheological Properties and Performance of Geopolymer-Modified Asphalt Binder and Mixtures. *Materials.* **2023**, *16, 1012*.
11. Moghaddam, T.B. Baaj, H. The use of compressible packing model and modified asphalt binders in high-modulus asphalt mixdesign. *Road Materials and Pavement Design*. **2020,***21, 1061–1077.*
12. Jizhe Zhang, Alex K. Apeagyei, Gordon D. Airey, James R.A. Grenfell. Influence of aggregate mineralogical composition on water resistance of aggregate–bitumen adhesion. *International Journal of Adhesion and Adhesives.* **2015**,*62, 45–54.*
13. Huang, G. Zhang, J. Hui, B. Zhang, H. Guan, Y. Guo, F. Li, Y. He, Y. Wang, D. Analysis of Modulus Properties of High-Modulus Asphalt Mixture and Its New Evaluation Index of Rutting Resistance. *Sustainability*. **2023**, *15, 7574.*
14. Zhang, H. Yang, X. Li, Y. Fu, Q. Rui, H. Laboratory Evaluation of Dynamic Characteristics of a New High-Modulus Asphalt Mixture. *Sustainability.* **2022**, *14, 11838.*
15. Chen, Y. Wang, H. Xu, S. You, Z. High modulus asphalt concrete: A state-of-the-art review. *Construction and Building Materials*. **2020**,*237, 117653.*
16. Hemmati, N. Vigneswaran, S. Kim, H.H. Lee, M.-S. Lee, S.-J. Laboratory Evaluation of Asphalt Binders Containing Styrene-Butadiene-Styrene (SBS) and Processed Oil. *Materials*. **2023**, *16, 1235.*
17. Weidong Huang, Naipeng Tang. Characterizing SBS modified asphalt with sulfur using multiple stress creep recovery test. *Construction and Building Materials*. **2015**,*93.*
18. Huang Junxian, Liu Yu, Muhammad Yaseen, Li Jia Qing, Ye Yuting, Li Jing, Li Zhuang, Pei Ruinan. Effect of glutaraldehyde-chitosan crosslinked graphene oxide on high temperature properties of SBS modified asphalt. *Construction and Building Materials*. **2022**,*357.*
19. Mugume, R. Kakoto, D. Effect of Inappropriate Binder Grade Selection on Initiation of Asphalt Pavement Cracking. *Sustainability*. **2020,** *12, 6099.*
20. Q. Li, H. Zhang, Z. Chen, Improvement of short-term aging resistance of styrenebutadiene rubber modified asphalt by Sasobit and epoxidized soybean oil. *Construction and Building Materials.* **2021**, *121870.*
21. J. D Angelo. Current Status of Superpave Binder Specification. *Road Materials and Pavement Design*. **2009,** *13–24.*
22. Matheus David Inocente Domingos , Adalberto Leandro Faxina. Accelerated short term ageing effects on the rheological properties of modifified bitumens with similar high PG grades. Road Materials and *Pavement Design.* **2015**, *469–480.*
23. Jian Zou, Reynalao Roque, Sanghyun Chun & George Lopp. Long-term fifield evaluation and analysis of top-down cracking for Superpave projects. *Road Materials and Pavement Design*. **2013**, *831–846.*
24. John D'Angelo, Fee Frank. Superpave binder tests and specifications: how have they performed in the real world? *Association of Asphalt Paving Technologists Proc*, **2000**, *69,697-713.*

25. Tao Wang, Feipeng Xiao, Serji Amirkhanian, Weidong Huang, Mulian Zheng. A review on low temperature performances of rubberized asphalt materials. *Construction and Building Materials*. **2017**,*145. 483–505.*
26. David A. Anderson, Donald W. Christensen, Hussain U. Bahia, Raj Dongre, M.G. Sharma, Charles E. Antle, Joe Button. Binder Characterization and Evaluation Volume 3: Physical Characterization. *Strategic Highway Research Program: Washington,* **1994**.
27. Tester, A.M.P. Testing for Fatigue Cracking in the Asphalt Mixture Performance Tester. *FHWA: Washington*, **2016**.
28. Roque Reynaldo, Yan Yu, Lopp George. Evaluation of the Cracking Performance of Asphalt Binders at Intermediate Temperatures. *University of Florida: Gainesville,* **2020**.
29. Yaning Qiao, Joao Santos, Anne M.K. Stoner, Gerardo Flinstch. Climate change impacts on asphalt road pavement construction and maintenance: An economic life cycle assessment of adaptation measures in the State of Virginia, United States. *Journal of Industrial Ecology*. **2020**,*24,2.*
30. Chao Wang, Xianxin Zhou, Guodong Gao. Study on Climate Impacts on Asphalt Pavement in Tibet, China. *Journal of Geoscience and Environment Protection.* **2019**,*49-59*.
31. American Asphalt Association, Reference manual for high performance asphalt pavement foundation, *Beijing People's Transport Press*. **2005.**
32. Ibrahim M. Asi. Performance evaluation of SUPERPAVE and Marshall asphalt mix designs to suite Jordan climatic and traffic conditions. *Construction and Building Materials*. **2006**,21,*8*.
33. Hossam F. Hassan, Ali Al-Nuaimi, Salim Al-Oraimi, Tufool M.A. Jafar. Development of asphalt binder performance grades for Omani climate. *Construction and Building Materials*. **2007**,*22,8.*
34. A.M.M. Saleh, Metwally A. Trad. Generation of asphalt performance grading map for Egypt based on the SUPERPAVE? program. *Construction and Building Materials.* **2011**,*25,5.*
35. M.Waseem Mirza , Zahid Abbas, Mujasim Ali Rizvi. Temperature Zoning of Pakistan for Asphalt Mix Design. *Pakistan Journal of Engineering and Applied Sciences*. **2011**,*49-60.*
36. Peerapong Jitsangiam, Prinya Chindaprasirt, Hamid Nikraz. An evaluation of the suitability of SUPERPAVE and Marshall asphalt mix designs as they relate to Thailand's climatic conditions. *Construction and Building Materials*. **2013**,*40.*
37. Hassan Awadat Salem, Djordje Uzelac, Bojan Matic. Temperature Zoning of Libya Desert for Asphalt Mix Design. *Applied Mechanics and Materials*. 2014,*3489,638-640.*
38. Francesco Viola, Clara Celauro. Effect of climate change on asphalt binder selection for road construction in Italy. *Transportation Research Part D*. **2015**,*37.*
39. Cota, J. Martínez-Lazcano, C. Montoya-Alcaraz, M. García, L. Mungaray-Moctezuma, A. Sánchez-Atondo, A. Improvement in Durability and Service of Asphalt Pavements through Regionalization Methods: A Case Study in Baja California, Mexico. *Sustainability*, **2022**, *14, 5123*.
40. Zhao Kaiwen, Ma Xianyong, Zhang Hongwei, Dong Zejiao. Performance zoning method of asphalt pavement in cold regions based on climate Indexes: A case study of Inner Mongolia. *Construction and Building Materials*,**2022,***361.*
41. JTG E20-2011, Standard Test Methods of Bitumen and Bituminous Mixtures for Highway Engineering. *Renmin Communication Press*. Beijing China,**2011**.
42. JTG F40-2004, The Chinese Technical Specification for Construction of Highway Asphalt Pavement. *Renmin Communication Press*. Beijing, China,**2004**.
43. T. W. Kennedy, G. Huber, E. Harrigan, R. Cominsky, C. Hughes, H. Quintus, J. Moulthrop Superior performing asphalt pavements (Superpave): The product of the SHRP asphalt research program, **1994**.